Hydrologic Controls on Aperiodic Spatial Organization in the Ridge Slough Patterned Landscape

Stephen T. Casey[1], Matthew J. Cohen[1,*], Subodh Acharya[1], David A. Kaplan[2] and James W. Jawitz[3]

1 – School of Forest Resources and Conservation, University of Florida, Gainesville FL

2 – Engineering School of Sustainable Infrastructure and Environment, Environmental Engineering Sciences Department, University of Florida, Gainesville FL

3 – Soil and Water Science Department, University of Florida, Gainesville, FL

* - Corresponding Author (email: mjc@ufl.edu; phone 352.846.3490)

Abstract

A century of hydrologic modification has altered the physical and biological drivers of landscape processes in the Everglades (Florida, USA). Restoring the ridge-slough patterned landscape, a dominant feature of the historical system, is a priority, but requires an understanding of pattern genesis and degradation mechanisms. Physical experiments to evaluate alternative pattern formation mechanisms are limited by the long time scales of peat accumulation and loss, necessitating model-based comparisons, where support for a particular mechanism is based on model replication of extant patterning and trajectories of degradation. However, multiple mechanisms yield a central feature of ridge-slough patterning (patch elongation in the direction of historical flow), limiting the utility of that characteristic for discriminating among alternatives. Using data from vegetation maps, we investigated the statistical features of ridge-slough spatial patterning (ridge density, patch perimeter, elongation, patch-size distributions, and spatial periodicity) to establish more rigorous criteria for evaluating model performance, and to inform controls on pattern variation across the contemporary system. Mean water depth explained significant variation in ridge density, total perimeter, and length:width ratios, illustrating important pattern response to existing hydrologic gradients. Two independent analyses (2-D periodograms and patch size distributions) provide strong evidence against regular patterning, with the landscape exhibiting neither a characteristic wavelength nor a characteristic patch size, both of which are expected under conditions that produce regular patterns. Rather, landscape properties suggest robust scale-free patterning, indicating genesis from the coupled effects of local facilitation and a global negative feedback operating uniformly at the landscape-scale. Critically, this challenges widespread invocation of meso-scale negative feedbacks for explaining ridge-slough pattern origins. These results help discern among genesis mechanisms

and provide an improved statistical description of the landscape that can be used to compare among model outputs, as well as to assess the success of future restoration projects.

Keywords: regular patterning, scale-free patterning, robust criticality, scaling relationships, ridge slough landscape, periodogram analysis, Everglades, wetland restoration.

1 Introduction

The coupling of ecosystem processes operating at different scales can cause vegetation communities to form a wide variety of spatial patterns (Borgogno et al., 2009), ranging from highly regular striping, stippling or maze-like patterns in woodland landscapes (Ludwig et al., 1999), tidal mud flats (Weerman et al., 2012), and boreal peatlands (Eppinga et al., 2010) to scale-free patterning in semi-arid landscapes (Kefi et al., 2007; Scanlon et al., 2007). The mechanisms that produce these patterns are integral to understanding landscape origins, and thus for predicting appropriate remedies where patterns and underlying processes have been degraded and require restoration. The spatial arrangement of vegetation on the landscape has long been viewed as a manifestation of the dominant interactions and drivers (Hutchinson, 1957; Levin, 1992), and the scales at which they operate. By quantifying this spatial arrangement we can make process-based inferences about the underlying mechanisms (Gardner et al., 1987; Turner, 2005).

The ridge-slough landscape comprised ~55 % of the pre-development Everglades in southern Florida (McVoy et al., 2011). However, processes that created, and in some places still maintain, the characteristic ridge-slough patterning are only partially understood (Science Coordination Team, 2003; Larsen et al., 2011; Cohen et al., 2011). The landscape pattern consists of flow-parallel bands of higher-elevation ridges dominated by emergent sedge sawgrass (*Cladium jamaicense*), interspersed within a matrix of lower-elevation sloughs (ca. 25 cm lower in the best conserved portions of the landscape; Watts et al., 2010), which contain a variety of submerged and emergent herbaceous macrophytes. The Everglades has undergone massive hydrologic modification through the construction of a system of levees and canals over the past century (Light and Dineen, 1994), and ensuing ecological degradation has prompted a complex,

expensive, and ambitious restoration effort. Because the ridge-slough landscape was so prevalent in the pre-development system, pattern restoration is a central priority (SCT 2003; McVoy et al., 2011). The mechanisms that control the emergence of patterning and explain variation in pattern geometry are thus integral to specifying hydrologic restoration objectives.

To understand the landscape processes that produce patterning, and by extension gain insight into how to restore them (Pickett and Cadenasso, 1995), requires a testable mechanistic framework for pattern genesis and maintenance. However, experiments to test alternative mechanisms are constrained by the spatial extent and time scales of peat accumulation responses. Paradoxically, compartmentalization by the extensive canal and levee system has created artificial gradients that are informative for assessing trajectories of landscape pattern degradation. Here we focus on Water Conservation Area 3 (WCA-3), located in the central Everglades, an area historically dominated by the ridge-slough landscape (Fig. 1), and where the best conserved patterning is found. The hydrologic gradient in WCA-3 spans from relatively dry (i.e., short hydroperiod) conditions in the north due to major canals that drain water to the southeast, to extended inundation (i.e., long hydroperiod) in the south and southeast due to impoundment caused by US41/Tamiami Trail (which runs orthogonal to flow) and the L-67 levee. The best conserved patterning (SCT, 2003; Watts et al. 2010) is found between these hydrologic extremes.

Several alternative hypotheses have been proposed to explain ridge slough patterns, and all have been evaluated using process-based models. The mechanisms invoked vary and include evaporative nutrient redistribution (Ross et al., 2006), flow-driven sediment redistribution from sloughs to ridges (Larsen et al., 2007; Larsen and Harvey 2011; Lago et al., 2010), ponding induced long-range inhibition (Cheng et al., 2011), self-optimization of patterning for discharge

and hydroperiod (Cohen et al., 2011; Kaplan et al., 2012; Heffernan et al., 2013), and a suite of mechanisms that couple pattern-hydroperiod effects with anisotropic local contagion processes (Acharya et al., 2015). Clearly, these mechanisms are not mutually exclusive, so process models have sought to explore the sufficiency of each alternative, while acknowledging the potential that multiple processes may overlap. One central criterion used to evaluate the models has been whether simulations can produce morphologies qualitatively consistent with the extant landscape (principally replicating the elongation of patches in the flow direction). To date, however, almost all models either accomplish (Ross et al., 2006; Larsen and Harvey, 2010; Lago et al., 2010; Cheng et al., 2011; Acharya et al., 2015) or strongly imply (Heffernan et al., 2013) this, limiting the ability to discriminate between pattern genesis mechanisms and highlighting the need for a more rigorous and quantitative characterization of landscape pattern.

To better characterize patterns in both the best conserved state and spanning a gradient of degradation requires spatial analyses that yield quantitative properties against which model outputs can be compared. Although numerous metrics have been developed to quantify different pattern attributes (Wu et al., 2007; Yuan et al., 2015), significant gaps in our understanding of how to interpret these metrics remain (Turner, 2001; Remmel and Csillag, 2003). Real landscapes clearly depart from regular Euclidean geometry, making characterization problematic in some cases (Mandelbrot, 1983). Likewise, changes in mapping procedures (e.g., grain size, extent, classification schemes) can yield significantly different metric values for the same landscape (Li and Wu, 2004). To remedy some of these issues, we focused on a set of relatively direct and easily interpreted metrics of fundamental aspects of the pattern, and used multiple maps produced with varying methods to rule out mapping-related artifacts. We were interested in three aspects of landscape patterning: density and shape statistics, patch-size distributions, and

spectral (i.e., pattern wavelength) characteristics. For each aspect, we explored the magnitude of site-to-site variation and the support for hydrologic control of that variation.

Density and shape statistics focus on the most basic and intuitive geometric properties of the landscape: areal coverage of the patch types (density), landscape pattern complexity (perimeter), and the degree of elongation. While inundation has been shown to control species composition (Givnish et al., 2008; Zweig and Kitchens, 2008; Todd et al., 2010), the relationship between hydrologic drivers and other aspects of landscape pattern remain relatively unknown, so this effort also serves as an inventory of hydrologic controls on pattern geometry.

Patch size distributions (i.e., frequency of different patch sizes) have been used in many systems to identify underlying landscape processes (e.g., Manor and Shnerb, 2008a; Kefi et al., 2011; Bowker and Maestre, 2012; Weerman et al., 2012). For example, regular patterning is associated with a characteristic patch size (Rietkerk and van de Koppel, 2008; von Hardenberg, 2010), arising in response to an inhibitory feedback operating at a particular spatial scale (van de Koppel and Crain, 2002) that limits patch expansion. Under these conditions, there should be a distinct mode in patch area distribution, or at least the absence of very large patches (Manor and Shnerb, 2008; von Hardenberg, 2010; Kefi et al., 2014). In contrast, patch size distributions that follow a power-law (i.e., $y=x^{\alpha}$, where α is a scaling parameter) lack a characteristic spatial scale (e.g., Scanlon et al., 2007) and may suggest genesis mechanisms that operate equally across scales. Correspondingly, power law distributions are often referred to as scale-free, in that the distribution form remains the same regardless of the measurement scale.

Scale-free distributions can arise via a number of mechanisms (Newman et al., 2005). In a landscape where grid cells are randomly occupied, patch distributions show relatively few large patches, up to a critical density (~0.59; known as the percolation threshold) at which patches

span the domain, yielding power-law area scaling. At densities slightly above and below the percolation threshold, area distributions depart from power-laws. The narrow range of density space over which scale-free area distributions emerge would seem to suggest that this mechanism is rare. However, some systems can endogenously maintain themselves near this critical point in a phenomenon referred to as self-organized criticality (Bak et al., 1989). This is accomplished through disturbance processes that propagate via patch contiguity (e.g., forest fires, see Drossel and Schwabl, 1992), maintaining patterns near the percolation threshold through a cycle of large-scale disturbance and slow recovery (Pascual and Guichard, 2005).

Alternatively, power-law scaling of patch areas can arise from the coupled action of local facilitation, which causes patches to expand, and competition for a global resource (Pascual et al., 2002; Scanlon et al., 2007) that ultimately limits the density of that patch type at the landscape scale. In contrast to regular patterning mechanisms, these feedback processes limit landscape-level patch density, but not the size of individual patches, leading to the creation, via local facilitation, of very large patches. This is known as robust criticality because power-law scaling in response can occur over a wide range of external conditions and patch densities, including densities well below the percolation threshold. Robust criticality has been noted in Everglades vegetation distributions (Foti et al., 2012), as well as in a variety of dryland vegetation patterns (Kefi et al., 2011). Widespread occurrence of both local facilitation and global resource competition in ecological systems suggests this process may operate in a multitude of landscapes.

Finally, spectral characteristics provide insights on the presence and wavelength of regular landscape pattern. Useful information about the scale at which spatial feedbacks operate in self-organized systems has been obtained by evaluating 2-dimensional pattern periodicity

(Couteron, 2002; Kefi et al., 2014). This is particularly important in the Everglades because the prevailing conceptual model for ridge-slough pattern genesis invokes interactions between spatial feedbacks operating on different characteristic scales, resulting in a pattern wavelength of approximately 150 m in the direction perpendicular to historical flow (SCT, 2003; Larsen et al., 2007; Watts et al., 2010). Several models (e.g. Ross et al., 2006; Lago et al., 2010; Cheng et al., 2011) produce distinctly periodic landscapes, which arise from the action of local facilitation feedbacks and, crucially, negative feedbacks on patch expansion that operate at a characteristic scale. In contrast, the feedback between hydroperiod and landscape geometry suggested by Cohen et al. (2011), enumerated by Heffernan et al. (2013), and tested at the landscape scale in Kaplan et al. (2012), operates at the global-scale, implying no characteristic spatial scale. To that end, we tested the hypothesis that the ridge-slough landscape is regularly patterned (i.e., exhibits a characteristic wavelength), consistent with scale-specific negative feedbacks, or whether the landscape lacks periodicity, consistent with scale-free feedbacks.

Together, these spatial analyses encompass a novel and rigorous set of metrics for improved quantification of observed and modeled landscape pattern. While developed to improve descriptions of the ridge-slough pattern, these metrics may also be useful for identifying pattern and discriminating genesis mechanisms in other patterned landscapes.

2 Methods

2.1 Vegetation and hydrologic data

We used multiple vegetation maps of the central Everglades, which vary in scale, extent, mapping schemes, and time frame. For all maps, we aggregated vegetation types into binary classes (reclassifcation scheme in Table S2) of ridges (*value* = 1) and sloughs (*value* = 0). Our

primary map (M1) was produced by the South Florida Water Management District (SFWMD) using 1:24 000-scale color infrared photos from September 1994 (Rutchey, 2005). This map was chosen due to its large, continuous spatial extent and fine mapping detail. The presence of small (<25 m^2) landscape features allowed us to rasterize polygons of dominant vegetation at 1 m resolution (i.e., 1×1 m cells). While the presence of small features does not imply map accuracy at that fine scale, it does imply loss of patch geometric detail with larger cells. Features at this scale can be subject to mapping error and artifacts, likely under-representing their prevalence. As such, patches below 100 m^2 were omitted from patch-level analyses.

We selected 33 6×6 km sites to span the range of current hydrological conditions (i.e., dry in northern areas to wet in southern areas; Fig. 1). We sought to maximize the number of sites with minimal overlap, while avoiding roads and canals. All sites except 20–22 and 32–33 were rotated to align with the prevailing direction of patch elongation (15° counterclockwise). Ridge cells were grouped into patches if they shared at least one edge with an adjacent ridge (i.e., a von Neumann neighborhood).

Within each site, *point-specific* daily average water depths at a grid spacing of 200 m were obtained from the Everglades Depth Estimation Network (EDEN) xyLocator (http://sofia.usgs.gov/eden/edenapps/xylocator.php). We note these water depths are spatially interpolated from a network of water elevation monitoring stations and, as such, represent only an estimate of actual conditions. *Site-specific* mean water depth (MWD) values were obtained by averaging all point-specific values in each site over the period of record from 1991–2010.

We used two additional maps (M2 and M3), which vary in spatial extent, resolution, and sampling date, to corroborate M1 analyses and test map resolution effects and temporal changes. M2 was generated from 1:24 000 scale aerial photographs taken in 2004 (RECOVER 2014) and

rasterized at 50 m resolution. M3 was generated from 1 m resolution digital orthophotos and rasterized at 1 m (Nungesser, 2011). Methodological details for both M2 and M3 are given as supplementary information.

2.2 Shape and density

We compared ridge density, edge density, and elongation across sites. Ridge density is the proportion of ridge area to site area, while edge density is total patch perimeter divided by site area. In order to measure elongation, E, we first identify individual lengths and widths (l and w, respectively) as any group of contiguous ridge cells (i.e. unbroken by slough cells) along a row or column. Elongation is the ratio of the mean of these contiguous row and column sections:

$$E = \frac{\frac{1}{n_c}\sum l}{\frac{1}{n_r}\sum w} = \frac{n_r}{n_c} \quad (1)$$

where n_r and n_c represent the number of contiguous rows and columns. Elongation simplifies to their ratio since the summation terms both yield the total number of ridge cells. Elongation metrics are sensitive to orientation differences between the grid and landscape features. Sites with tortuous flow paths or a poorly aligned grid will underestimate E. We provide estimates of grid alignment with feature orientation as a mean patch angle, $\bar{A}_p$, where A_p is the angle between the grid y axis and the major axis of an ellipse with the same second moment as the patch.

Hydrologic trends were identified by regressing MWD against site-level metrics, and were considered statistically significant at $p<0.05$. For analyses that are highly dependent on mapping resolution (i.e., edge density), we omit M1 sites north of Interstate-75, as these were mapped using significantly lower resolution than those to the south (Rutchey, 2005). Because elongation values are dominated by the domain shape at very high ridge densities, we omitted sites where ridge density exceeded 0.8.

2.3 Patch size distributions

Patch size scaling properties were evaluated by comparing empirical distributions to several candidate models. Patch size distributions can be described in terms of their complementary cumulative distribution function (CCDF), which gives the probability that the area of an observed patch is greater than or equal to a given area, *x*. Preliminary analyses showed that empirical CCDFs exhibited extremely heavy tails consistent with power laws, but only above a minimum cutoff, below which patches were less abundant and the CCDFs were rounded. This form is in relative agreement with both the Generalized Pareto (GP) and truncated lognormal distributions. The GP is given by its CCDF as

$$P(x) = \begin{cases} \left(1 + \frac{k(x - x_{\min})}{\delta}\right)^{-\frac{1}{k}} & \text{for } k \neq 0 \\ \exp\left(-\frac{x - x_{\min}}{\delta}\right) & \text{for } k = 0 \end{cases} \quad (2)$$

for $x \geq x_{min}$ when $k \geq 0$, and for $x_{min} \leq x \leq (x_{min} - \delta/k)$ when $k < 0$. The GP reduces to the exponential distribution when $k = 0$ and $x_{min} = 0$, and reduces to a power-function when $k > 0$ and $x_{min} = \delta/k$. For $k > 0$ and $x_{min} < \delta/k$ the GP shows exponential-like behavior for low values of x, while the tail asymptotically approaches a power law for $x >> x_{min}$. Within this range of parameters, δ indicates the curvature in the upper end of the distribution (higher values correspond to greater curvature and hence, relatively fewer small patches), while k indicates the scaling properties of the tail, such that for $x >> x_{min}$, the power-law scaling exponent α approaches $\alpha^* = (1 + 1/k)$(Pisarenko and Sornette, 2003). Where the GP fits the data well, we can use the estimated parameters as general information about patch size scaling properties. The CCDF for a truncated lognormal distribution uses the mean ($\mu_{\ln x}$) and standard deviation ($\sigma_{\ln x}$) of $\ln(x)$.

$$P(x) = \frac{\mathrm{erf}\left(\frac{\sqrt{2}[\mu_{\ln x} - \ln(x)]}{2\sigma_{\ln x}}\right) + 1}{\mathrm{erf}\left(\frac{\sqrt{2}[\mu_{\ln x} - \ln(x_{min})]}{2\sigma_{\ln x}}\right) + 1} \qquad x \geq x_{min} \qquad (3)$$

We compared empirical distributions to synthetic data sets from Monte Carlo simulations (n = 20,000 per model) and compared candididate distributions based on log-likelihood ratios and significance values (Clauset et al., 2009). Distribution testing details are given in SI.

2.4 Spectral characteristics

Spectral characteristics of the ridge-slough landscape were evaluated from 2-D periodograms generated following the methods of Mugglestone and Renshaw (1998). In brief, we constructed a discrete 2-D Fourier transform (available in most computational software packages) for each binary vegetation map (Kefi et al., 2014), and then took the absolute value to obtain the real number component. The resulting 2-D periodogram (i.e. spectral density) is a grid representing the magnitude of cosine and sine waves of possible wavenumbers (i.e. spatial frequencies), and orientations to the spectrum. Values were averaged across all orientations in equally spaced wavenumber bins to generate radial spectra (r spectra), which indicate the relative spectral density for each corresponding wavenumber bin. Local maxima indicate dominant wavelengths, and thus suggest the presence of spatial periodicity (Couteron, 2002; Kefi et al., 2014), or regular patterning. The absence of local maxima indicates the landscape is aperiodic. Because the ridge-slough pattern has been described as regular in the direction orthogonal to flow, we complemented our omnidirectional analysis with a directional r spectrum derived from the spectral density observed at $\pm 10°$ from perpendicular to the main axis of pattern elongation.

3 Results

3.1 Visual comparisons

Visual inspection of the vegetation maps reveals a remarkable range of pattern morphology (Fig. 1). Ridges in northwestern sites (1–5, a) show pronounced striping, which is less apparent in southern sites (18–22, h, i), where ridges appear more elliptical. Eastern sites located below I-75 (5, 9, 13, 14, 17, 28–33, b, f, g, i, j) show fine-scale speckling and disaggregation, with sites 14, 28 and 29 appearing random, with faint outlines of historic pattern.

Individual ridges exhibit numerous connections between adjacent elongated portions, with larger patches forming complex webs composed of multiple individual elements. Although this behavior is apparent in all sites, it appears to be density dependent, with most of the landscape spanned by one large patch in denser sites (e.g., M1: 2, 5, 8, 9, 11–13, 23–28, 30–33; M2: 1, 2, 4, 5, 8, 9, 12, 23–28, 30–33; M3: a, b, d, j). Within sites, large patches are always more web-like than smaller ones, which appear more distinctly separated.

3.2 Density and shape

Ridge density was negatively correlated to MWD (Fig. 2a; $R^2 = 0.38$, $p = 0.0002$). Deviation from this association was similar across maps and related to geographic position. Specifically, ridge densities in the eastern half of the domain (sites 9, 13, 14, 17, 23–33; b, f, g, i, j) were consistently higher than in the west, suggesting a strong east–west control on density. The correlation between MWD and ridge density increased markedly when sites were partitioned into east and west blocks (east: $R^2 = 0.81$, $p < 0.0001$; west: $R^2 = 0.61$, $p = 0.0004$). Based on recent aerial imagery, low ridge density in site 1 is a misclassification of sparse sawgrass prairies as slough; that site was omitted from regression analyses.

Site-level elongation was also strongly correlated to MWD (Fig. 2b; $R^2 = 0.65$, $p < 0.0001$). Sites with ridge densities greater than 0.8 showed elongation values much lower than this trend. Average patch orientations ($\bar{A}_p$) indicate consistency between the grid and features (i.e., $\bar{A}_p$ values close to zero; Table S1). In sites with values of $|\bar{A}_p| \geq 5°$) (e.g., M1: 1, 22; M2: 9, 18, 25, 27, 29, 31; M3: d, g), may possess underestimated elongation may be underestimated due to mismatch between patch orientation and map orientation. Finally, edge density was strongly correlated to MWD, indicating greater perimeter at deeper sites (Fig. 2c; $R^2 = 0.79$, $p < 0.0001$).

3.3 Patch size distributions

Patch area distributions were consistent with the Generalized Pareto distribution (Fig. 3c), with 16 of 25 sites passing GP Monte Carlo tests for M1 and 4 of 9 passing for M3 (Table S1). The majority of sites that were not significant contained extremely large patches, but had little deviation in the rest of the distribution; in some cases (e.g., sites 2, 5, 8, 9, 11, 12, 13, 28, 31; a, d, j) the largest patch was over an order of magnitude larger than predicted based on the GP distribution. All these sites with extremely large patches have ridge densities above or very close to the percolation threshold of a square lattice (~0.59, Stauffer, 1995). Above this percolation threshold, the largest patch becomes "over-connected", suggesting that failure of Monte Carlo tests within this group may be density driven, rather than a result of an underlying patterning mechanism. Note that these sites are largely located in the north and eastern sections of the study area, a region typified by high ridge densities. The log-normal distribution was significant in only 4 of 25 sites for M1 and 2 of 9 sites for M3. Although these sites (15, 16, 19, 21; c and h) showed slight rounding in the extreme tail, log-likelihood ratios were not different enough to distinguish between the two candidate distributions (Table S1).

Within each map, GP parameters were remarkably consistent across sites, with almost constant estimates of k and δ for sites that passed Monte Carlo tests (Table S1). Area scaling in the tail of the distribution is illustrated by α^* (analogous to the scaling exponent of a power-law distribution) = 1.77 ± 0.06 for M1 and 1.87 ± 0.13 for M3. The δ parameter indicates how sharply the distribution head deviates from a power-law, with larger values indicating that smaller patch areas are exceedingly rare. For M1 and M3, δ = 474 ± 88 and 1490 ± 219; these differences are likely due to map resolution, with M3 under-representing smaller patches.

3.4 Spectral characteristics

We found no evidence of peridocity from the omnidirectional r spectra. The absence of peak values other than the smallest wavenumber indicates that no dominant pattern wavelength exists, a finding consistent across hydrologic conditions and pattern morphologies (Fig. 3a). Directional r spectra are consistent with the omnidirectional r spectra, but are noisier due to reduced sample sizes (Fig. 3b). Spearman correlations, ρ, show the r spectra monotonically decreased across all sites (Table S1), consistent with maximum spatial variation at the largest scale, and decreasing consistently at smaller scales. For M1, each site had $\rho < -0.999$ and $\rho < -0.99$ for the full and directional r spectra, respectively.

The r spectra were roughly linear in log-log space, and were approximated by a power–law relationship. For the full r spectra, all sites in M1 had $R^2 \geq 0.98$; $p < 0.0001$; $\alpha = -1.31 \pm 0.03$, while for the directional r spectra, $R^2 \geq 0.97$; $p < 0.0001$; $\alpha = -1.35 \pm 0.03$ (see Table S1). Slight rounding at the extreme ends was observed; rounding at high wavenumbers is consistent with the loss of fine-scale features due to a low sampling resolution, while rounding at low wavenumbers arises from a spatial extent of the domains, and is consistent with undersampling

of large features at low wavenumbers. Some highly disturbed sites (e.g. 9, 13, 14, 17, 22, 24, 25, 30, 31, 33) showed slightly more rounded *r* spectra but still lacked any evidence of periodicity.

4 Discussion

4.1 Water depth controls pattern attributes

Our results provide strong observational support for water depth as a dominant control on several key shape and density properties of the ridge-slough landscape. The observed decline in ridge abundance with MWD is consistent with conceptual models that predict that changes in water levels precipitate transitions between ridge and slough by modifying production and respiration dynamics (Givnish et al., 2008; Watts et al., 2010) and inducing state changes in vegetation composition (Zweig et al., 2008). The implication that these dynamics differ in eastern and western sections of the study area was unexpected, and points to unexplained controls on ridge expansion. The largest difference between the east and west trends occurs at low water depths, indicating that this control is most pronounced in drier sites. In short, the deviation seen in eastern sites represents a shifting of the relationship to favor sawgrass expansion in extremely dry sites, rather than a general reduction of the hydrologic limitation (since deep sites remain the least affected).

Mean water depth also exerted strong control on ridge-slough pattern shape. The most salient features of the pattern, elongation and perimeter, both showed strong dependence on MWD, with maximum elongation observed at low to intermediate water depths and minimum perimeter values at low water depths. This is consistent with ridge features fragmenting into smaller, less elongated patches under deeper water conditions, a finding previously observed anecdotally (McVoy et al., 2011) and in the spatial statistics of soil elevation (Watts et al., 2010).

Likewise, sites with very low MWD show a significant loss of pattern, with ridge densities approaching unity and elongation values that are largely isotropic. The coherent response of these pattern features to hydrologic modification suggests promise for their use as restoration performance measures (Yuan et al., 2015).

In this work we provide support for hydrological controls on ridge-slough pattern shape; however landscape patterning (specifically ridge density and elongation) has also been shown to exert reciprocal control on regional hydrology (Kaplan et al., 2012). Loss of sloughs in sites with very low MWD alters drainage characteristics. Coupled to observations of patch fragmentation in sites with higher water depths, these results strongly reinforce the commanding role of hydrology in maintaining landscape pattern, indicating that reversal of modern hydrologic modification is paramount for ongoing restoration.

4.2 The ridge-slough landscape is aperiodic and scale-free

Both spatial periodogram results and patch size distributions strongly suggest the ridge-slough landscape pattern is aperiodic, a marked departure from extensive literature qualitatively describing the pattern as periodic (SCT 2003; Wetzel et al., 2005; Ross et al., 2006; Larsen, 2007; Givnish et al., 2008; Larsen and Harvey, 2010; Lago et al., 2010; Watts et al., 2010; Cheng et al., 2011; Nungesser, 2011; Sullivan et al., 2014). Because negative feedbacks operating at a characteristic spatial scale result in regular patterning (Rietkerk and Van de Koppel, 2008), aperiodic patterning in the ridge-slough landscape implies the absence of such feedbacks, ruling out many of the mechanisms invoked to explain pattern formation (Borgogno et al., 2009).

Instead, the observation that patch size distributions uniformly follow power-law scaling, suggests a scale-free patterning process. While power-law scaling can be produced via several

391 mechanisms (Newman et al., 2005), our results can be used to rule out some alternatives. For
392 example, power-law scaling of patch areas can arise in systems near the percolation threshold
393 (i.e., at criticality), which occurs within a relatively narrow region of patch density. Observed
394 patch area scaling in our study occurs across a wide range of patch densities, suggesting robust
395 criticality that comports with Foti et al. (2012), who observed similar power-law scaling
396 behavior over a wide range of vegetation types and densities.

397 Caution is warranted when using contemporary aerial imagery to infer pre-drainage
398 landscape conditions; the first aerials were taken ~65 years after Everglades drainage began.
399 Several pattern attributes (e.g., density, perimeter) may adjust readily with hydrologic
400 modification, and while some areas remain largely unchanged since initial imagery was obtained,
401 pattern in many other areas has degraded, sometimes entirely (Wu et al. 2006, Nungesser 2011).
402 However, pattern properties that are relatively invariant with hydrologic modification (e.g. r
403 spectrum, power-law scaling of patch areas) are more likely to reflect pre-drainage conditions. In
404 contrast, measures that vary with hydrologic modification are useful for understanding landscape
405 responses to hydrologic forcing, but may be less informative for inferring pre-drainage
406 conditions and long-term processes such as landscape formation.

407 Self-organized criticality can also produce power-law scaling at varying densities (i.e., far
408 from the percolation threshold), but requires large temporal variation in ridge density as the
409 system endogenously readjusts towards criticality following disturbances (Pascual and Guichard,
410 2005). Recent paleoecological evidence (Bernhardt and Willard, 2010) suggests that ridge-
411 slough configurations and densities have remained relatively stable since initial formation 2700
412 years before present, which is inconsistent with the requisite temporal variation in density.
413 Moreover, no documented disturbance regime exhibits the characteristic separation of time

scales between growth and disturbance associated with self-organized criticality. While peat fires could be invoked, there is little evidence for widespread incidence and large-scale impacts of these prior to modern hydrologic modification (McVoy et al., 2011).

Rather, smooth variation in ridge densities along environmental gradients is consistent with robust criticality, wherein local facilitation induces clustering (i.e., patch growth) while a global limitation maintains landscape heterogeneity (Pascual and Guichard, 2005). Although robust criticality is typically suggested in isotropic landscapes, Acharya et al. (2015) recently showed that anisotropy in the local facilitation kernel of a robust criticality model can produce directional banding without periodicity, yielding simulated ridge-slough patterns with high statistical and visual fidelity to the observed landscape. Local facilitation may take the form of autogenic peat accretion (Larsen et al., 2007), clonal propagation of sawgrass (Brewer, 1996), nutrient accumulation dynamics (Cohen et al., 2009, Larsen et al. 2015), or local seed dispersal, although the relative importance and directionality of these mechanisms remains unknown (Acharya et al., 2015). Screening possible mechanisms for anisotropic local facilation emerges from our analysis as a priority for future investigations.

Several candidate processes could limit patch expansion in the ridge slough landscape. Each implies a distinct spatial pattern geometry, and we can use the extant scale-free and aperiodic geometry to evaluate their respective plausibilities. A key distinction between limiting processes that produce periodic versus scale-free patterning is the spatial range over which the limiting factor acts (Manor and Shnerb, 2008a; von Hardenberg, 2010). When the limiting effect of patch expansion locally is spread uniformly across the landscape, the effect is considered global or uniform. Conversely, when the limiting effect act in a more localized manner, limitation gradients can develop and produce periodic patterning.

Phosphorus limitation and sediment transport mechanisms are both potentially important feedbacks on patch expansion. While phosphorus is strongly limiting of primary production in the Everglades (Noe et al., 2001), and can be dramatically enriched in tree-islands (Wetzel et al. 2009) and ridges (Ross et al. 2006) via multiple mechanisms, this process of local enrichment and depletion is inconsistent with robust criticality. Indeed, the presence of strong local phosphorus gradients indicates that limitation feedbacks are distinctly local, and not spread uniformly across the landscape. If phosphorus limitation were the dominant control, the result would be regular patterning. Similarly, sediment transport mechanisms (Larsen et al., 2007; Lago et al., 2010) yield a balance between entrainment and deposition governed by focused flow in sloughs, the velocity of which is controlled by cross-sectional occlusion of flow by ridges. Because patch expansion and contraction is controlled by local heterogeneity in flow velocity, this suggests an inhibitory feedback operating at a limited spatial scale.

Water level (and hydroperiod) is another potential feedback on patch expansion. Our observations of water depth control on ridge density comport with numerous studies (Givnish et al., 2008; Zwieg and Kitchens, 2008; Todd et al., 2012) suggesting ridges are significantly impacted by water depths. Moreover, pattern geometry strongly influences landscape hydrology (Kaplan et al. 2012, Acharya et al. 2015). As ridges expand into adjacent sloughs, they displace water and alter landscape flow capacity, causing regional water levels to increase (Kaplan et al., 2012), and creating a negative feedback that likely limits further ridge expansion (Cohen et al. 2011). Because water depths equilibrate quickly, local patch expansion effects are distributed rapidly and relatively evenly across the landscape. This consistent with the global limitation necessary to create the observed aperiodic and scale-free pattern. Therefore, water depth effects are strong candidates for the requisite global feedback necessary for ridge-slough formation.

The ridge-slough landscape pattern has emerged as a key measure of restoration performance in one of the largest and most ambitious ecosystem management endeavors ever. Enumeration of spatial pattern statistical features is a prerequisite for assessing landscape condition and for comparing models with alternative landscape genesis mechanisms. Our results inform the metrics for comparison between real and simulated landscape patterns, and provide insights into the controls on pattern variation across the contemporary system. Given the potentially significant differences in water management implied by comparative genesis explanations, these metrics of real and simulated landscapes are important for restoration planning and assessment.

Our results also indicate that elongated landscape features do not necessarily require pattern periodicity, suggesting that spatial structures in numerous ecosystems may have been misclassified as regularly patterned, and that aperiodic banding may be more prevalent than the literature suggests. Invoking robust criticality and anisotropic local contagion, as in Acharya et al. (2015), may be of general value for explaining aperiodic banding in other settings.

References

Acharya, S., Kaplan, D.A., Casey, S., Cohen, M.J., and Jawitz, J.W.: Coupled local facilitation and global hydrologic inhibition drive landscape geometry in a patterned peatland, Hydrology and Earth System Sciences, 19(5), 2133-2144, 2015.

Bak, P., Tang, C., and Wiesenfeld, K.: Self-organized criticality, Phys. Rev. A, 38, 364–374, 1989.

Borgogno, F., D'Odorico, P., Laio, F., and Ridolfi, L.: Mathematical models of vegetation pattern formation in ecohydrology, Rev. Geophys., 47, RG1005, 2009.

Brewer, J. S.: Site differences in the clone structure of an emergent sedge, *Cladium jamaicense*, Aquat. Bot., 55, 79–91, 1996.

Cheng, Y., Stieglitz, M., Turk, G., and Engel, V.: Effects of anisotropy on pattern formation in wetland ecosystems, Geophys. Res. Lett., 38, 2011.

Clauset, A., Shalizi, C. R., and Newman, M. E.: Power-law distributions in empirical data, SIAM Rev., 51, 661–703, 2009.

Cohen, M. J., Osborne, T. Z., Lamsal, S. J., and Clark, M. W.: Regional Distribution of Soil Nutrients-Hierarchical Soil Nutrient Mapping for Improved Ecosystem Change Detection, South Florida Water Management District, West Palm Beach, Florida, USA, 91 pp., 2009.

Cohen, M.J., Watts, D.L., Heffernan, J.B., and Osborne T.Z.: Reciprocal biotic control on hydrology, nutrient gradients and landform in the Greater Everglades, Crit. Rev. Environ. Sci. Technol., 41, 395-429, 2011.

Couteron, P.: Quantifying change in patterned semi-arid vegetation by Fourier analysis of digitized aerial photographs, Int. J. Remote Sens., 23, 3407–3425, 2002.

Eppinga, M. B., Rietkerk, M., Borren, W., Lapshina, E., Bleuten, W., and Wassen, M.: Regular surface patterning of peatlands: confronting theory with field data, Ecosystems, 11, 520–536, 2008.

Eppinga, M. B., Rietkerk, M., Belyea, L., Nilsson, M., Ruiter, P., and Wassen, M.: Resource contrast in patterned peatlands increases along a climatic gradient, Ecology, 91 (8), 2344-2355, 2010.

Foti, R., del Jesus, M., Rinaldo, A., and Rodriguez-Iturbe, I.: Hydroperiod regime controls the organization of plant species in wetlands, P. Natl. Acad. Sci. USA, 109, 19596–19600, 2012.

Givnish, T. J., Volin, J. C., Owen, V. D., Volin, V. C., Muss, J. D., and Glaser, P. H.: Vegetation differentiation in the patterned landscape of the central Everglades: importance of local and landscape drivers, Global Ecol. Biogeogr., 17, 384–402, 2008.

Heffernan, J. B., Watts, D. L., and Cohen, M. J.: Discharge competence and pattern formation in peatlands: a meta-ecosystem model of the everglades ridge-slough landscape, PloS one, 8, e64174, 2013.

Kaplan, D. A., Paudel, R., Cohen, M. J., and Jawitz, J. W.: Orientation matters: patch anisotropy controls discharge competence and hydroperiod in a patterned peatland, Geophys. Res. Lett., 39, L17401, 2012.

Kéfi, S., Rietkerk, M., Alados, C. L., Pueyo, Y., Papanastasis, V. P., ElAich, A., and De Ruiter, P. C.: Spatial vegetation patterns and imminent desertification in Mediterranean arid ecosystems, Nature, 449, 213–217, 2007.

Kéfi, S., Rietkerk, M., Roy, M., Franc, A., De Ruiter, P. C., and Pascual, M.: Robust scaling in ecosystems and the meltdown of patch size distributions before extinction, Ecol. Lett., 14, 29–35, 2011.

Kéfi, S., Guttal, V., Brock, W. A., Carpenter, S. R., Ellison, A. M., Livina, V. N., Seekell, D. A., Scheffer, M., van Nes, E. H., and Dakos, V.: Early warning signals of ecological transitions: methods for spatial patterns, PloS one, 9, e92097, 2014.

Lago, M. E., Miralles-Wilhelm, F., Mahmoudi, M., and Engel, V.: Numerical modeling of the effects of water flow, sediment transport and vegetation growth on the spatiotemporal patterning of the ridge and slough landscape of the Everglades wetland, Adv. Water Resour., 33, 1268–1278, 2010.

Larsen, L.G., Harvey, J.W., and Maglio, M.M: Mechanisms of nutrient retention and its relation to flow connectivity in river–floodplain corridors, Freshwater Science 34, 187-205, 2015.

Larsen, L. G. and Harvey, J. W.: How vegetation and sediment transport feedbacks drive landscape change in the Everglades and wetlands worldwide, Am. Nat., 176, E66–E79, 2010.

Larsen, L. G. and Harvey, J. W.: Modeling of hydroecological feedbacks predicts distinct classes of landscape pattern, process, and restoration potential in shallow aquatic ecosystems, Geomorphology, 126.3, 279-296, 2011.

Larsen, L. G., Harvey, J. W., and Crimaldi, J. P.: A delicate balance: ecohydrological feedbacks governing landscape morphology in a lotic peatland, Ecol. Monogr., 77, 591–614, 2007.

Larsen, L. G., Aumen, N., Bernhardt, C., Engel, V., Givnish, T., Hagerthey, S., Harvey, J., Leonard, L., McCormick, P., McVoy, C., Noe, G., Nungesser, M., Rutchey, K., Sklar, F., Troxler, T., Volin, J., and Willard, D.: Recent and historic drivers of landscape change in the Everglades ridge, slough, and tree island mosaic, Crit. Rev. Env. Sci. Tec., 41, 344–381, 2011.

Li, H. and Wu, J.: Use and misuse of landscape indices, Landscape Ecol., 19, 389–399, 2004.

Light, S. S. and Dineen, J. W.: Water Control in the Everglades: a Historical Perspective, Everglades: the Ecosystem and its Restoration, St. Lucie Press, Delray Beach, Florida, 47–84, 1994.

Limpert, E., Stahel, W. A., and Abbt, M.: Log-normal distributions across the sciences: keys and clues, Bioscience, 51, 341–352, 2001.

Ludwig, J. A., Tongway, D. J., and Marsden, S. G.: Stripes, strands, or stipples: modelling the influence of three landscape banding patterns on resource capture and productivity in semi-arid woodlands, Australia, Catena, 37, 257–273, 1999.

552 Mandelbrot, B. B.: The Fractal Geometry of Nature, Freeman, New York, 1983.
553 Manor, A. and Shnerb, N. M.: Facilitation, competition, and vegetation patchiness: from scale
554 free distribution to patterns, J. Theor. Biol., 253, 838–842, 2008a.
555 Manor, A. and Shnerb, N. M.: Origin of Pareto-like spatial distributions in ecosystems, Phys.
556 Rev. Lett., 101, 268104, 2008b.
557 McVoy, C., Park Said, W., Obeysekera, J., VanArman, J., and Dreschel, T.: Landscapes and
558 Hydrology of the Predrainage Everglades, University Press of Florida, Gainesville, FL,
559 2011.
560 Mugglestone, M. A. and Renshaw, E.: Detection of geological lineations on aerial photographs
561 using two-dimensional spectral analysis, Comput. Geosci., 24, 771–784, 1998.
562 Newman, M. E.: Power laws, Pareto distributions and Zipf's law, Contemp. Phys., 46, 323–351,
563 2005.
564 Noe, G. B., Childers, D. L., and Jones, R. D.: Phosphorus biogeochemistry and the impact of
565 phosphorus enrichment: why is the Everglades so unique?, Ecosystems, 4, 603–624,
566 2001.
567 Nungesser, M. K.: Reading the landscape: temporal and spatial changes in a patterned peatland,
568 Wetl. Ecol. Manag., 19, 475–493, 2011.
569 Pascual, M. and Guichard, F.: Criticality and disturbance in spatial ecological systems, Trends
570 Ecol. Evol., 20, 88–95, 2005.
571 Pascual, M., Roy, M., Guichard, F., and Flierl, G.: Cluster size distributions: signatures of self–
572 organization in spatial ecologies, Philos. T. R. Soc. B, 357, 657–666, 2002.
573 Pickett, S. T. and Cadenasso, M. L.: Landscape ecology: spatial heterogeneity in ecological
574 systems, Science, 269, 331–334, 1995.
575 Pisarenko, V. F. and Sornette, D.: Characterization of the frequency of extreme earthquake
576 events by the generalized Pareto distribution, Pure Appl. Geophys., 160, 2343–2364,
577 2003.
578 RECOVER: 2014 System Status Report, Restoration Coordination and Verification Program, c/o
579 US Army Corps of Engineers, Jacksonville, FL, and South Florida Water Management
580 District, West Palm Beach, FL, 2014.
581 Remmel, T. K. and Csillag, F.: When are two landscape pattern indices significantly different?,
582 J. Geogr. Syst., 5, 331–351, 2003.
583 Rietkerk, M. and Van de Koppel, J.: Regular pattern formation in real ecosystems, Trends Ecol.
584 Evol., 23, 169–175, 2008.
585 Ross, M. S., Mitchell-Bruker, S., Sah, J. P., Stothoff, S., Ruiz, P. L., Reed, D. L., Jayachandran,
586 K., and Coultas, C. L.: Interaction of hydrology and nutrient limitation in the Ridge and
587 Slough landscape of the southern Everglades, Hydrobiologia, 569, 37–59, 2006.
588 Rutchey, K., Vilchek, L., and Love, M.: Development of a vegetation map for Water
589 Conservation Area 3, Technical Publication ERA Number 421, South Florida Water
590 Management District, West Palm Beach, FL, USA, 2005.

Scanlon, T. M., Caylor, K. K., Levin, S. A., & Rodriguez-Iturbe, I. (2007). Positive feedbacks promote power-law clustering of Kalahari vegetation.Nature, 449(7159), 209-212.

Science Coordination Team: The Role of Flow in the Everglades Ridge and Slough Landscape, South Florida Ecosystem Restoration Working Group, West Palm Beach, FL, 2003.

Stauffer, D. and Aharony, A.: Introduction to percolation theory, Taylor and Francis, London, 1991.

Sullivan, P. L., Price, R. M., Miralles-Wilhelm, F., Ross, M. S., Scinto, L. J., Dreschel, T. W., Sklar, F. H., and Cline, E.: The role of recharge and evapotranspiration as hydraulic drivers of ion concentrations in shallow groundwater on Everglades tree islands, Florida (USA), Hydrol. Process., 28, 293–304, 2014.

Todd, M. J., Muneepeerakul, R., Pumo, D., Azaele, S., Miralles-Wilhelm, F., Rinaldo, A., and Rodriguez-Iturbe, I.: Hydrological drivers of wetland vegetation community distribution within Everglades National Park, Florida, Adv. Water Resour., 33, 1279–1289, 2010.

Turner, M. G.: Landscape Ecology in Theory and Practice: Pattern and Process, Springer-Verlag, New York, 2001.

Turner, M. G.: Landscape ecology: what is the state of the science?, Annu. Rev. Ecol. Evol. S., 36, 319–344, 2005.

von Hardenberg, J., Kletter, A. Y., Yizhaq, H., Nathan, J., and Meron, E.: Periodic vs. scale-free patterns in dryland vegetation, P. R. Soc. B, 277, 1771–1776, 2010.

Watts, D. L., Cohen, M. J., Heffernan, J. B., and Osborne, T. Z.: Hydrologic modification and the loss of self-organized patterning in the ridge–slough mosaic of the Everglades, Ecosystems, 13, 813–827, 2010.

Weerman, E. J., Van Belzen, J., Rietkerk, M., Temmerman, S., Kéfi, S., Herman, P. M. J., and de Koppel, J. V.: Changes in diatom patch-size distribution and degradation in a spatially self-organized intertidal mudflat ecosystem, Ecology, 93, 608–618, 2012.

Wetzel, P. R., van der Valk, A. G., Newman, S., Gawlik, D. E., Troxler Gann, T., Coronado-Molina, C. A., Childers, D. L., and Sklar, F. H.: Maintaining tree islands in the Florida Everglades: nutrient redistribution is the key, Front. Ecol. Environ., 3, 370–376, 2005.

Wetzel, P. R., van der Valk, A. G., Newman, S., Coronado, C. A., Troxler-Gann, T. G., Childers, D. L., Orem, W. H., and Sklar, F. H.: Heterogeneity of phosphorus distribution in a patterned landscape, the Florida Everglades, Plant Ecol., 200, 83–90, 2009.

Wu, Y., Wang, N., Rutchey, K.: An analysis of spatial complexity of ridge and slough patterns in the Everglades ecosystem, Ecol. Complex., 3, 183–192, 2006.

Yuan, J., Cohen, M. J., Kaplan, D. A., Acharya, S., Larsen, L. G., and Nungesser, M. K.: Linking metrics of landscape pattern to hydrological process in a lotic wetland, Landscape Ecol., in review, 2015.

Zweig, C. L. and Kitchens, W. M.: Effects of landscape gradients on wetland vegetation communities: information for large-scale restoration, Wetlands, 28, 2008.

631

Figure Legends

Figure 1: Study area and site locations, including major roads, canals, and levees for the primary map (M1). Sites spanning the pattern gradient in WCA3 are shown in the bottom panel. Two additional maps (supplementary information) were used to corroborate the primary results.

Figure 2: **(a)** Ridge density is negatively correlated with mean water depth. Eastern sites (blue) show consistently higher ridge densities than those in the west (black). Trends associated with east–west segregation (dashed lines) show much stronger relationships than the composite trend (solid line). Site 1 was omitted due to possible misclassification. **(b)** Site elongation shows a strong negative relationship with mean water depth. Sites with ridge densities greater than 0.8 (indicated in grey) were omitted from regressions and show elongation values lower than expected from this trend. **(c)** Edge density is positively correlated to mean water depth indicating higher perimeters in deeper sites. Sites indicated in grey were mapped at lower resolution, and were omitted from regressions. The relationships observed for site elongation and edge density are both consistent with patches becoming disaggregated with increased water depth.

Figure 3: **(a)** Omnidirectional *r* spectra for the full angular range (0° - 180°) monotonically decreased with no evidence of peaks, indicating strictly aperiodic behavior. The r-spectra across sites approximately follows a power-law (red line), with rounding at both extremes attributed to mapping extent and resolution issues. **(b)** Directional *r* spectra limited to $\pm 10°$ in the direction perpendicular to the pattern also indicate aperiodic patterning, even when inference is constrained to the direction of presumed regularity. **(c)** Across sites, patch size distributions are well described by the generalized Pareto distribution (red lines). Sites with high ridge densities (e.g. sites 2, 5 and 25) have maximum patch sizes much greater than expected from the GP distribution. Conversely, sites in the deeply inundated southern section of WCA-3A (e.g. site 20) show slightly steeper tails, consistent with the lognormal distribution (blue lines), although the deviation is not significant enough to rule out the GP for these sites.

673

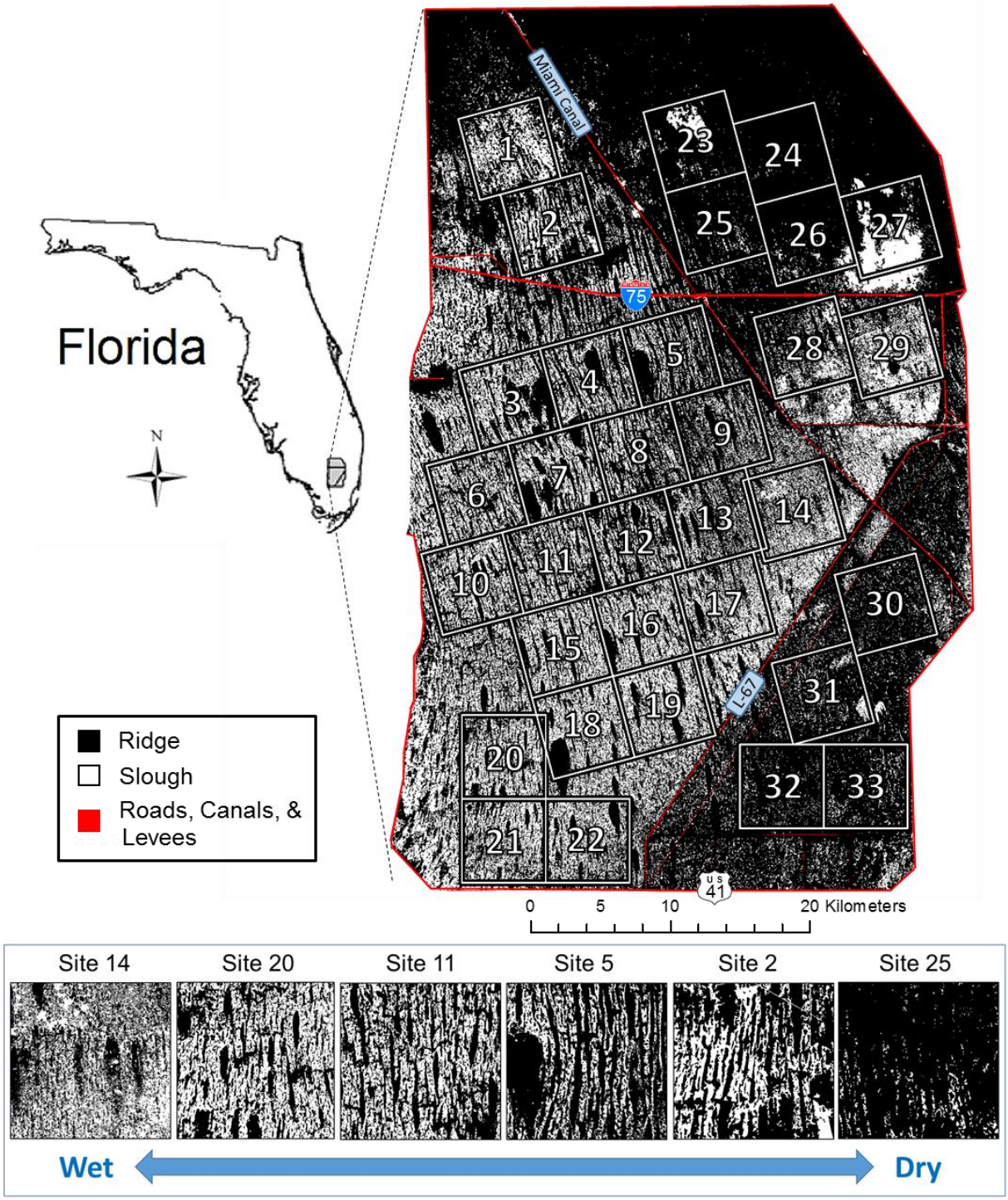

674
675
676 Figure 1

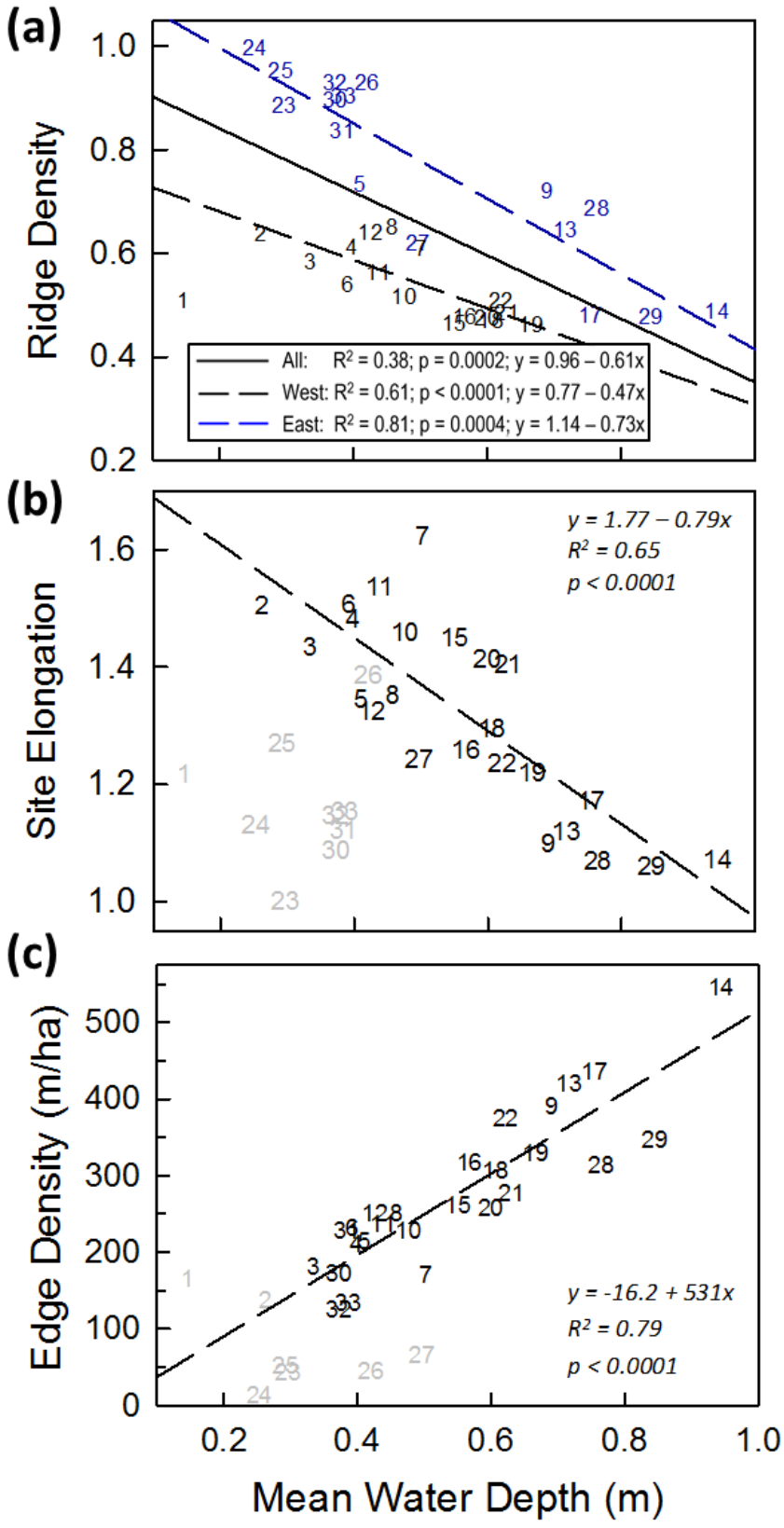

678 Figure 2
679

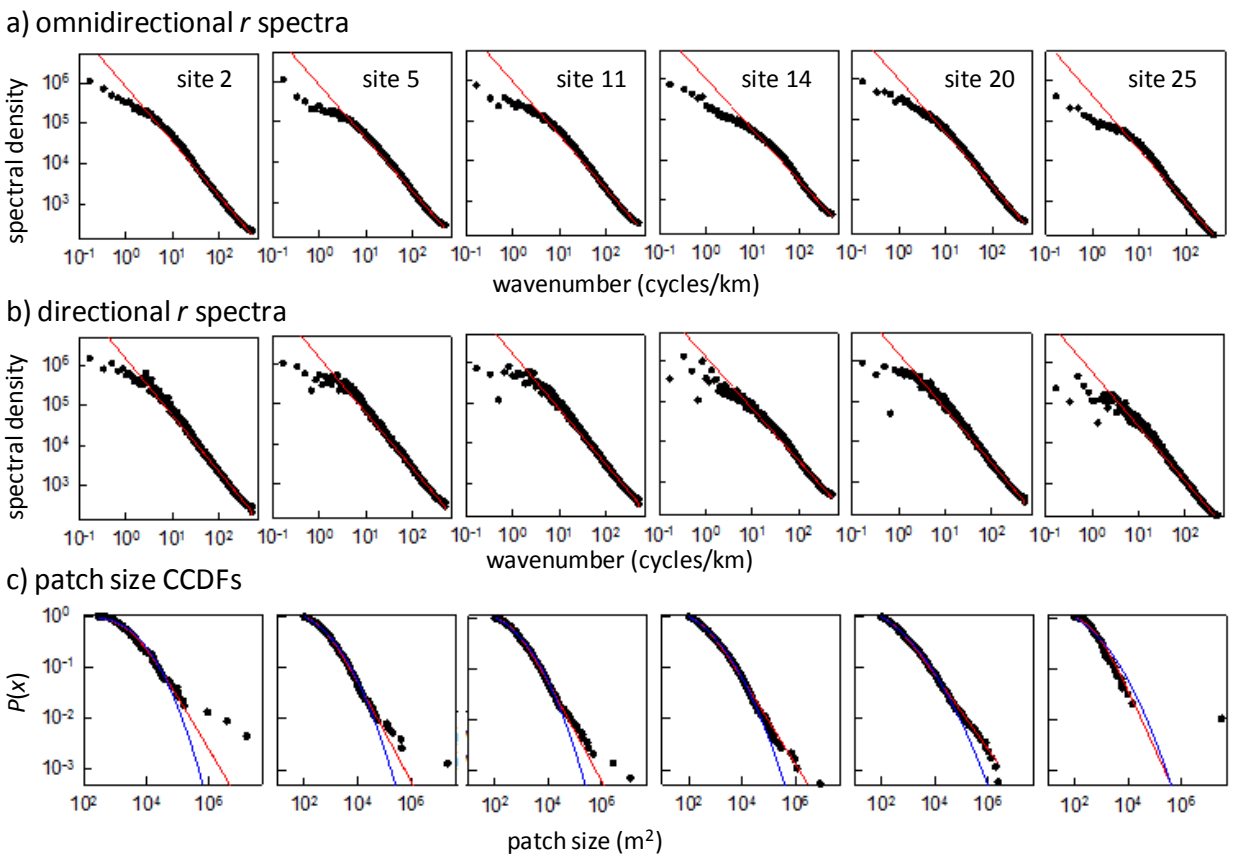
a) omnidirectional r spectra
site 2
site 5
site 11
site 14
site 20
site 25
spectral density
wavenumber (cycles/km)
b) directional r spectra
spectral density
wavenumber (cycles/km)
c) patch size CCDFs
P(x)
patch size (m²)

Figure 3